Gyrokinetic electrostatic turbulence close to marginality in the Wendelstein 7-X stellarator

Alessandro Zocco ,[1] Linda Podavini ,[1,2,3] José Manuel Garcìa-Regaña,[4] Michael Barnes,[5] Felix I. Parra ,[6]
A. Mishchenko,[1] and Per Helander[1]

[1]*Max-Planck-Institut für Plasmaphysik, Wendelsteinstraße 1, D-17491 Greifswald, Germany*
[2]*Università Milano Bicocca, Dipartimento di Fisica Giuseppe Occhialini, Piazza della Scienza, 3 20126 Milano, Italy*
[3]*Institut für Physik, Universität Greifswald, 17489 Greifswald, Germany*
[4]*Laboratorio Nacional de Fusión, CIEMAT, 28040 Madrid, Spain*
[5]*Rudolf Peierls Centre for Theoretical Physics, University of Oxford, Oxford OX1 3NP, United Kingdom*
[6]*Princeton Plasma Physics Laboratory, 100 Stellarator Road, Princeton, New Jersey 08540, USA*

The transition from strong (fluidlike) to nearly marginal (Floquet-type) regimes of ion-temperature-gradient (ITG) driven turbulence is studied in the stellarator Wendelstein 7-X by means of numerical simulations. Close to marginality, extended (along magnetic field lines) linearly unstable modes are dominant, even in the presence of kinetic electrons, and provide a drive that results in finite turbulent transport. A total suppression of turbulence above the linear stability threshold of the ITG modes, commonly present in tokamaks and known as the "Dimits shift," is not observed. We show that this is mostly due to the peculiar radial structure of marginal turbulence, which is more localized than in the fluid case and therefore less likely to be stabilized by shearing flows.

Introduction. The magnetic confinement fusion device Wendelstein 7-X (W7-X) has successfully proved that collisional losses in stellarators can be substantially reduced through magnetic-field optimization [1–3], thus setting an important milestone, among many [4], in the quest for a stellarator fusion reactor. The reduction of neoclassical transport (as such collisional losses are known in magnetically confined plasmas), however, does not imply that stellarators are immune to turbulent losses. And indeed, comparisons of neoclassical predictions with experimental measurements (as well as impurity transport measurements [5,6]) suggest that most of the energy losses are due to turbulence [1]. Perhaps the most striking evidence of turbulence-dominated losses in W7-X is the existence of a cap on the achievable core ion temperature [7]. This phenomenon manifests itself through an exacerbation of fluctuation levels with an increasing electron temperature [7], and is understood, among other things, in terms of a "τ effect" on the threshold for the destabilization of the ion-temperature-gradient (ITG) driven linear instability [8], which is believed to cause anomalous core transport [9]. Here, $\tau = T_i/T_e$ is the ratio of the ion to electron temperature, respectively. While knowledge of the linear threshold of the ITG instability is useful for understanding turbulent transport, its character at temperature gradients close to the stability threshold is largely unknown. In this Letter, we characterize

turbulence regimes that dominate transport in such experimentally relevant conditions. Our study is performed with the gyrokinetic flux-tube code STELLA [10], a semi-implicit code which allows one to retain electron kinetic effects and yet avoid the restrictions on time step of explicit algorithms due to the large mass difference between electrons and ions, thus making the simulations of saturated kinetic turbulence close to marginality relatively affordable. It is found that for experimentally relevant conditions, gyrokinetic turbulence in W7-X is of the ITG Floquet type [8,11] and not of the traditional fluid type [12,13]. Spectra of fluctuations, in some relevant time frame, can follow known scalings derived for far from marginality tokamak turbulence [10]. We observe no evidence of a sudden transition to regimes of highly turbulent transport for increasing temperature gradients, below which turbulence is suppressed by zonal flows [14]. That is, the turbulent heat flux does not show a "Dimits shift" [15]. We link this behavior to the peculiar radial structure of turbulence close to marginality, which is narrower than in the fluid regime, and thus naturally less prone to $\mathbf{E} \times \mathbf{B}$ shearing stabilization due to zonal flows.

Formulation and numerical setting. The turbulence we study is caused by fluctuations in the electrostatic potential, φ, which is determined by the quasineutrality condition

$$\sum_s e_s \int d^3\mathbf{v} F_{0s} \frac{e_s \varphi}{T_{0s}} = \sum_s e_s \int d^3\mathbf{v} \sum_{\mathbf{k}} e^{i\mathbf{k}\cdot\mathbf{r}} J_0(a_s) \delta G_{s\mathbf{k}},$$

(1)

which involves all species s, where charge is denoted by e_s, and temperature by T_{0s}. Here, F_{0s} is the equilibrium distribution function (taken to be Maxwellian), and thus the total density is $n_s = \int d^3\mathbf{v} f_s$, with $f_s = F_{0s} +$

$\delta f_s \equiv F_{0s}[1 - e_s \varphi(\mathbf{r}, t)/T_{0s}] + \delta G_s(\mathbf{R}_s, \mu, \mathcal{E}, t) + \mathcal{O}(\epsilon^2)$, and $\delta f_s/F_{0s} \sim k_\parallel/k_\perp \sim \omega/\Omega_s \sim \rho_* \equiv \epsilon \ll 1$, where $k_\parallel$ and $k_\perp$ are wave vectors along and across the equilibrium magnetic field, and ρ_* is the ratio of the Larmor radius to a characteristic macroscopic length. Here, $\mathbf{R}_s = \mathbf{r} + \mathbf{v}_\perp \times \hat{\mathbf{b}}/\Omega_s$ is the gyrocenter position, where $\mathbf{r}$ is the particle position, $\Omega_s = e_s B/(m_s c)$, $\hat{\mathbf{b}} = \mathbf{B}/B$, with $\mathbf{B}$ the equilibrium magnetic field, and $\mu = v_\perp^2/(2B)$, $\mathcal{E} = v^2/2$ the velocity-space coordinates. The Bessel function, $J_0 = J_0(a_s)$, with $a_s = 2B\mu k_\perp^2/\Omega_s^2$, relates the Fourier transform of δG_s with respect to $\mathbf{R}_s$ to its Fourier transform with respect to $\mathbf{r}$. The function δG_s satisfies the nonlinear gyrokinetic equation [16]

$$\left(\frac{\partial}{\partial t} + v_\parallel \nabla_\parallel + \mathbf{v}_{d,s} \cdot \nabla \right) \delta G_s$$
$$= \frac{e_s F_{0s}}{T_{0s}} \frac{\partial}{\partial t} \langle \varphi \rangle_{\mathbf{R}_s} - \frac{c}{B} \mathbf{b} \cdot \nabla \langle \varphi \rangle_{\mathbf{R}_s} \times \nabla F_{0s}$$
$$- \frac{c}{B} \mathbf{b} \cdot \nabla \langle \varphi \rangle_{\mathbf{R}_s} \times \nabla \delta G, \qquad (2)$$

where, $\langle \varphi \rangle_{\mathbf{R}_s} = \sum_{\mathbf{k}} \langle \varphi \rangle_{\mathbf{R}_s, \mathbf{k}} \exp(i \mathbf{k} \cdot \mathbf{R}_s)$, with $\langle \varphi \rangle_{\mathbf{R}_s, \mathbf{k}} = J_0(a_s) \varphi_{\mathbf{k}}$ the gyroaveraged electrostatic potential, $\nabla = \partial/\partial \mathbf{R}_s$, and $\mathbf{v}_{d_s} = -v_\parallel \mathbf{b} \times \nabla(v_\parallel/\Omega_s)$, $v_\parallel = \sqrt{2(\mathcal{E} - B\mu)}$. We simulate two kinetic species with equal temperatures at the radial location $r/a = 0.7$, for a high mirror configuration, as in [8]. Here, a is the average minor radius and $r = \sqrt{\psi/\psi_{LCFS}}$, $\psi = \psi_t/(2\pi)$ with ψ_t the toroidal magnetic flux, and ψ_{LCFS} its value at the last closed flux surface. Flux-tube coordinates are used, and thus $\mathbf{B} = \nabla \alpha \times \nabla \psi$, where α labels field lines, z is a general toroidal angle which measures the distance along the magnetic field, and $\mathbf{k}_\perp = k_\psi \nabla \psi + k_\alpha \nabla \alpha$. Furthermore, $\hat{s} = d(\ln q)/d \ln(\psi) = -0.1249$, where $q = 1.103$ measures the pitch of the field lines. We consider flat density and electron temperature profiles. Linearly, we confirm that electron kinetics does not substantially alter the original picture of Ref. [8]. Thus we can identify a transition for the ion-temperature-gradient (ITG) driven instability, where the branch driven by the magnetic field curvature, at moderate temperature gradients, gets progressively stabilized as the temperature gradient is reduced, and a background of (Floquet-type) modes emerges [see Fig. 1, where we plot the eigenvalues and eigenfunctions of the most unstable wavelengths; see, also, Figs. 2(c) and 2(d)]. While, for large temperature gradients, one toroidal turn of the flux tube is more than enough to resolve the mode structure, for the Floquet-ITG instability, one needs a flux tube that is significantly longer (see Fig. 1, inset, where we simulate three toroidal turns). Importantly, nearly marginal ITG modes feature a rather low critical gradient for destabilization, which occurs already for $a/L_T < 1$, where $1/L_T = T_{0i}^{-1} dT_{0i}/dx$ [8,17]. This could be an issue if such low critical gradients would also persist nonlinearly, potentially limiting performance. The ultimate scope of this Letter is to evaluate the nonlinear transport due to these modes.

Nonlinear results. We choose two temperature gradients across the transition described above (see Fig. 1: $a/L_T = 2$ and $a/L_T = 0.9$), and set up a series of nonlinear simulations of the Fourier transform of Eq. (2), solving for $\delta G_{\mathbf{k}}$, where $\delta G = \sum_{k_x, k_y} \delta G_{\mathbf{k}} \exp(i k_x x + i k_y y)$, with
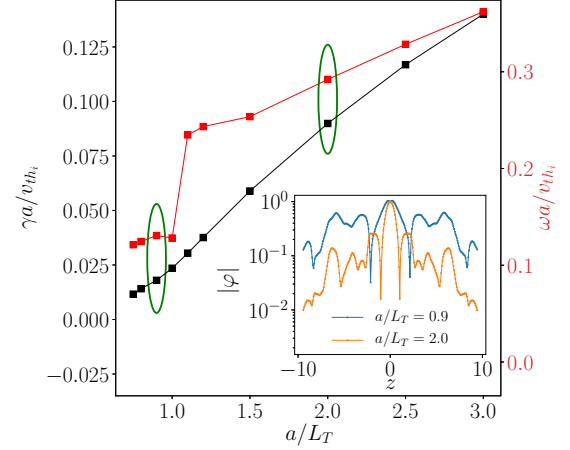
FIG. 1. Growth rate and frequency for the most unstable ITG mode as a function of the temperature normalized gradient scale a/L_T. In the circles, the two cases are analyzed nonlinearly. Inset: linear eigenfunctions. Fluidlike ($a/L_T > 1$) and Floquet-type ($a/L_T < 1$) modes.

$x = (dx/d\psi)(\psi - \psi_0)$, $y = (dy/d\alpha)(\alpha - \alpha_0)$, $dx/d\psi = a/(2\sqrt{\psi \psi_{LCFS}})$, and $dy/d\alpha = a\sqrt{\psi/\psi_{LCFS}}$. We consider $\rho_i k_{x,max} \equiv \hat{k}_{x,max} \approx 2.13$, $\hat{k}_{y,max} = 2.5$, with resolutions $\Delta k_x/k_{x,max} = 1/61$, $\Delta k_y/k_{y,max} = 1/51$, where $\rho_i = v_{thi}/\Omega_i$ is the ion Larmor radius. For the variable z, we choose to solve for two toroidal turns, which are computationally more affordable but allow us to capture the broad structure of the linear eigenfunction. We then take at least $n_z = 128$ points. In velocity space, we have $n_\mu = 24$ and $n_{v_\parallel} = 64$, for $\mu_{max} \approx 5$ and $v_{\parallel,max} = 3$, in normalized units. In Fig. 2, we identify three key instants of the time evolution of fluctuations: the first, in which zonal structures ($\hat{k}_y = 0$) reach a minimum, after a transient phase; the second, in which the amplitude of zonal structures equals that of the main drive of turbulence; the third, in which fluctuations reach a maximum and then saturate. We then analyze the Fourier spectra of the time-averaged, field-line-averaged fluctuations, in these time intervals. We also report the primary linear instability that causes turbulence, for $a/L_T = 2$. (fluidlike) and $a/L_T = 0.9$ (Floquet-type), respectively. In the first case, we observe an isotropic structure at $(\hat{k}_x, \hat{k}_y) = (0., 1.05)$, commonly present in axisymmetric simulations, accompanied by two distinct lobes at $(\hat{k}_x, \hat{k}_y) = (\pm 0.837, 1.05)$. Such structures at finite k_x have been extensively investigated. More of them can be found by extending the k_x domain, but the additional ones become less and less prominent as k_x is increased. They persist for more extended flux tubes. For smaller gradients, linearly, we observe a pronounced reduction of the mode at $(\hat{k}_x, \hat{k}_y) = (0., 1.05)$, but not of the finite-$\hat{k}_x$ lobes, which are actually reinforced by the new extended (along the line; see the inset of Fig. 1) primary mode, and slightly shifted to higher $\hat{k}_y$. The new primary mode, interestingly, develops within the same $\hat{k}_y$ band that is manifestly stable for large gradients (around $\hat{k}_y = 0.5$), and shows a narrower radial structure (since it is broader in $\hat{k}_x$ space). After this first phase, the evolution of primary modes departs from the linear one, and enters a presaturation phase, culminating at the
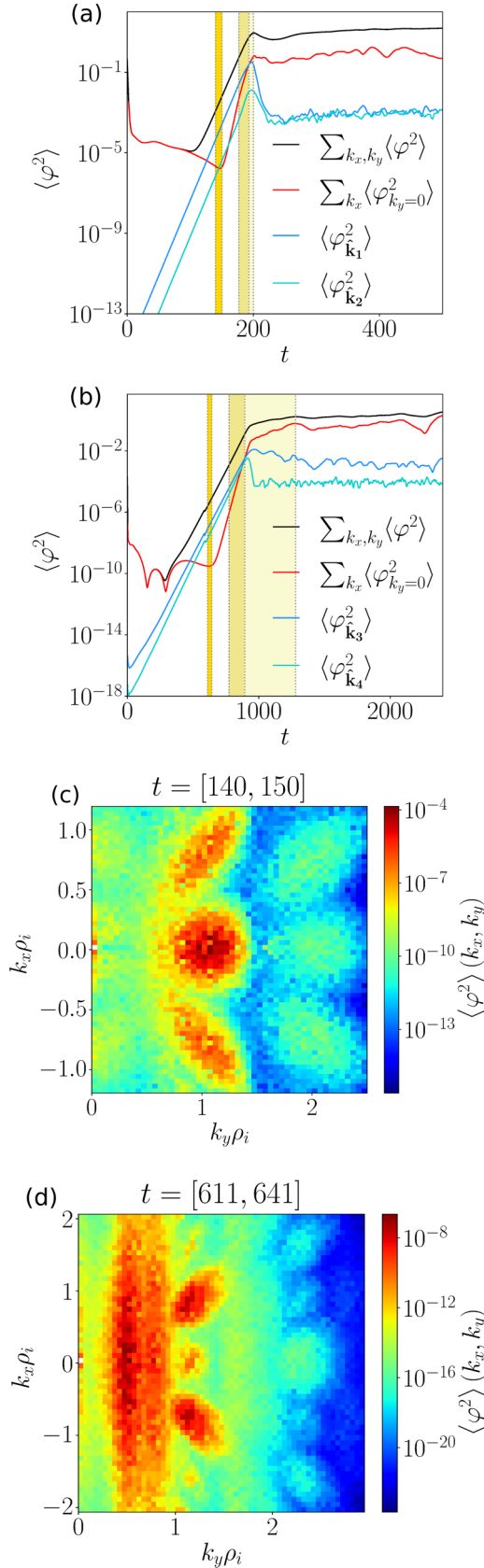
FIG. 2. Time traces of averaged electrostatic fluctuations and spectra in the linear regime for (a), (c) $a/L_T = 2$. and (b), (d) $a/L_T = 0.9$. Here, $\rho_i \mathbf{k}_1 = (0., 1.05)$, $\rho_i \mathbf{k}_2 = (0.837, 1.05)$, $\rho_i \mathbf{k}_3 = (0.14, 0.5)$, $\rho_i \mathbf{k}_4 = (0.71, 1.05)$.
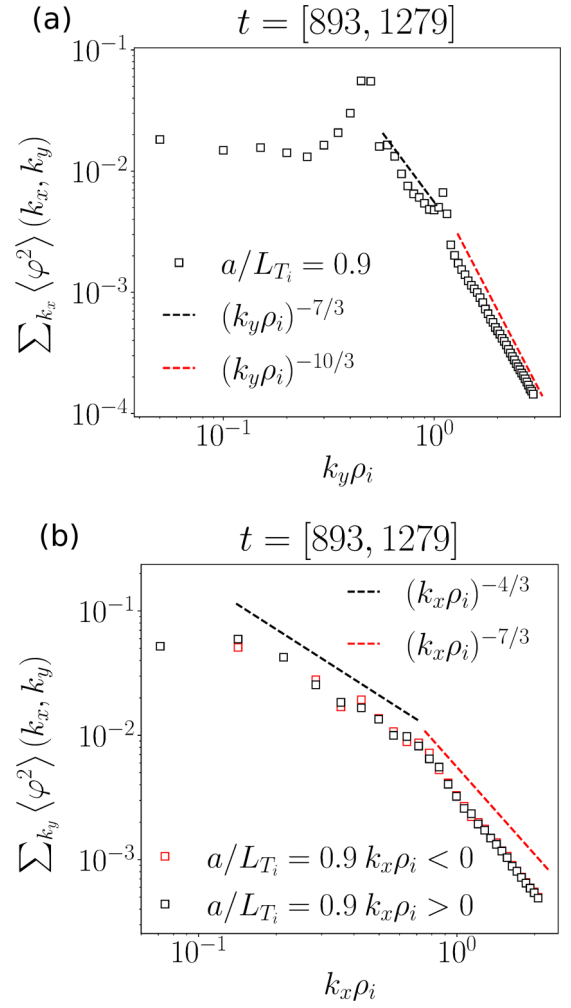
FIG. 3. Scalings for spectra of fluctuations in the saturating regimes. Here, $a/L_T = 0.9$.

instant in which the zonal modes' amplitudes ($\hat{k}_y = 0$) reach the amplitude of the primary drive ($t = 193$ and $t = 893$, for $a/L_T = 2$ and $a/L_T = 0.9$). This is the moment in which zonal flows start playing a prominent role and saturation takes place. In the fluid case, the finite-$\hat{k}_x$ lobes get isotropized, and their amplitude is significantly reduced. Two key actors remain mostly active: the primary at $(\hat{k}_x, \hat{k}_y) = (0., 1.05)$ and the zonal modes at $\hat{k}_y = 0$. Very importantly, both the primary and its "lobe" are violently suppressed by up to four orders of magnitude [time trace of $\langle \varphi^2_{\hat{\mathbf{k}}_1} \rangle$ and $\langle \varphi^2_{\hat{\mathbf{k}}_2} \rangle$ of Fig. 2(a)]. For $a/L_T = 0.9$, a similar time-trace analysis reveals that the zonal flow less efficiently suppresses the Floquet primary at $\hat{\mathbf{k}}_3 = (0.14, 0.5)$, which shows a much longer decaying time and larger saturation level than the lobe mode at $\hat{\mathbf{k}}_4 = (0.71, 1.05)$. It is in this time frame, which alone lasts longer than the whole simulation at $a/L_T = 2$, that marginal turbulence sets up a steep sub-ρ_i inertial range (Fig. 3). Here, while the sub-ρ_i range is limited, the steepness of the spectrum and the number of data points allow us to determine an unambiguous transition at the ion Larmor scale. Indeed, for $k_y \rho_i \lesssim 1$ (long wavelengths), the $\sum_{k_x} \varphi^2_{k_x,k_y} \sim (k_y \rho_i)^{-7/3}$ scaling [18] is observed. The

same scaling was observed elsewhere [19] and proposed as specific to W7-X turbulence. However, for $k_y \rho_i \gtrsim 1$, we find that the W7-X spectrum closely follows the sub-ρ_i scaling $\sum_{k_x} \varphi_{k_x,k_y}^2 \sim (k_y \rho_i)^{-10/3}$ of Ref. [20]. This type of scaling was also observed in Ref. [19] and proposed as specific to the turbulence in the quasihelically symmetric stellarator HSX. In our case, the sub-ρ_i variation of $\sum_{k_x} \varphi_{k_x,k_y}^2$ occurs over two orders of magnitude. A quantitative interpolation gives $\sum_{k_x} \varphi_{k_x,k_y}^2 \sim (k_y \rho_i)^{-\alpha}$, with $\alpha = 10.104 \pm 0.276$. In the long-wavelength limit ($k_y \rho_i \leqslant 1$), the range over which we observe the scaling $(k_y \rho_i)^{-7/3}$ is limited. This is due to the fact that the actual theoretical prediction requires a stretching of the scaling variables with a/L_T, which would considerably extend the inertial range for large a/L_T. For the specific case of Fig. 3, we have $a/L_T = 0.9$, whence the limited inertial range. Nevertheless, a clear sign of the long-wavelength result is still observable even for moderate gradients. The observation of the sub-ρ_i scaling must be put in the broader context of a general steepening of turbulence spectra with decreasing temperature gradients. The spectrum in Fig. 3(a) fully determines the primary source of turbulence that needs to be suppressed by zonal flows in order to achieve a steady state. Once this occurs, the steepening of the scaling persists but in a less pronounced fashion, being incompatible with any scaling shallower than $(k_y \rho_i)^{-9/3}$. A transition at scales somewhat larger than the ion Larmor radius is seen for the radial spectra of fluctuations [Fig. 3(b)]. At present, there is no theoretical explanation for these k_x scalings, which are reported for the sake of completeness.

Dimits shift? We have seen that close to marginality, in W7-X, the primary source of turbulence is less prone to zonal flow suppression. It is known that the effectiveness of zonal flows is a key aspect in enabling a nonlinear up-shift of the threshold at which, nonlinearly, microinstabilities give turbulent transport [14,21]. In tokamaks, for realistic conditions [22], a transition to finite turbulence levels can be less abrupt than originally found [15]. However, a substantial shift is always observed. We show here why this does not occur in W7-X. To verify how well zonal flows suppress the primary modes for our case studies, we performed a series of numerical experiments where the zonal flow was artificially suppressed [23] in the $\mathbf{E} \times \mathbf{B}$ nonlinearity. When this is done, in the nonlinear phase, fluctuations indeed grow faster and to larger amplitudes. The importance of this effect decreases with decreasing a/L_T. We systematically analyze the time traces of amplitudes and compare their values reached at the first maximum occurring after emerging from the presaturation regime. We must stress that in this way, we are assessing the effectiveness of the zonal flow in saturating the turbulence caused by the primary mode, and *not* the relative importance of the saturated amplitudes. The ratio $r(t) = |\varphi_{w/o}^2|/|\varphi_w^2|$ of the modulus squared of the amplitudes evaluated, following the prescribed procedure, is therefore measured. We find $r = \{5.1, 4.7, 3.3\}$ for $a/L_T = \{4, 2, 0.9\}$. We ascribe the lack of effectiveness in the turbulence suppression by zonal flows to the radial structure of turbulence itself. Indeed, we measure the average radial correlation lengths $\overline{\Delta x} = \{5.0, 2.9\}$ for $a/L_T = \{2, 0.9\}$. Here, $\overline{\Delta x} = \int_0^\infty \mathcal{C}(\Delta x) d(\Delta x)$, where
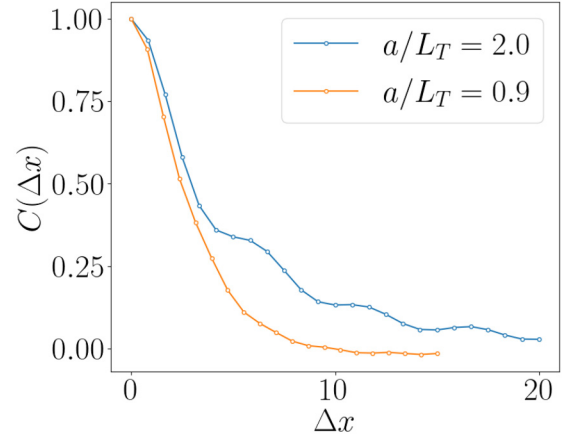
FIG. 4. The turbulence radial correlation function for $a/L_T = 2$, ($t > 400$) and $a/L_T = 0.9$ ($t > 1279$). Time windows refer to Fig. 2. Turbulence is radially more localized for smaller gradients.

$\mathcal{C}(\Delta x) = (\int dt dx dy dz |\varphi|^2)^{-1} \int dt dx dy dz \varphi(x)\varphi(x + \Delta x)$ is the turbulence radial correlation function, evaluated from the data (Fig. 4).

These two facts allow Floquet-type modes to give finite transport. In Fig. 5, we plot the turbulent heat flux $Q = V^{-1} \int d^3\mathbf{r} \int d^3\mathbf{v}(\mathbf{v}_E \cdot \nabla x)(m_i v^2/2)\delta f_i$, in normalized units, as a function of the ion temperature gradient. We notice that for $a/L_T = 2$, the value $Q/Q_{GB} \approx 4$ agrees well with the $\rho_i/a = 1/150$ result of a full surface W7-X calculation [24]. We verified that this saturation level does not depend on the length of the flux tube. Previous works regarding turbulence saturation in W7-X have studied $a/L_T \gtrsim 3$ [19]. Large values of a/L_T are out of the range of experimental ones. See Fig. 7(j) in Ref. [7] and Fig. 6 of [9], where in fact $a/L_T \lesssim 2$ in a large portion of the plasma volume. We can only observe a smooth transition to regimes where turbulent transport is considerably higher for higher gradients, but, for low gradients, turbulence is never completely suppressed. This result is somewhat similar to what is observed in quasihelical symmetric stellarators [25,26], but different from tokamaks. Behind our curve in Fig. 5, there is a weakly damped (by zonal flows), radially localized turbulence whose primary is the Floquet ITG. A direct comparison of the spectrum of the heat flux and
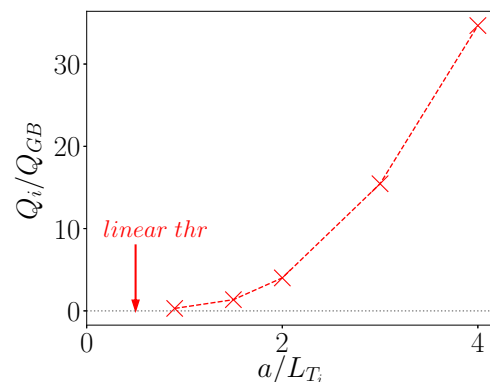
FIG. 5. Turbulent heat flux vs ion temperature gradient. Normalized units.
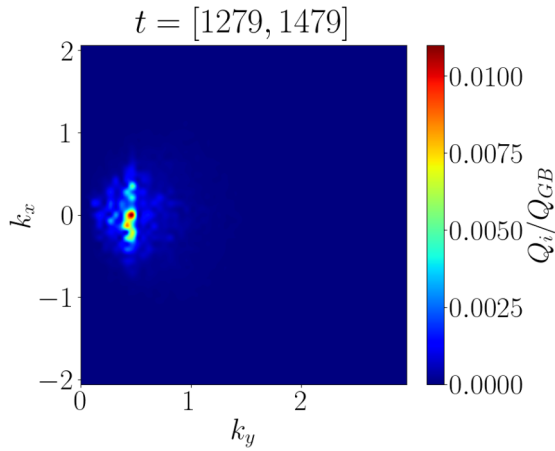
FIG. 6. The turbulent heat flux for $a/L_T = 0.9$ ($t > 1279$). Time windows refer to Fig. 2. The direct correlation with the primary source of turbulence of Fig. 2(d) stems from the lack of effectiveness of suppression from the zonal flow

electrostatic fluctuations corroborates this picture; see Fig. 6 which compares favorably with Fig. 2.

Discussion and conclusion. In this work, we have characterized the ion-temperature-gradient (ITG) driven turbulence in the stellarator Wendelstein 7-X, for the experimentally relevant situation in which temperature gradients approach the linear instability threshold from above. Even in the presence of kinetic electrons, a background of extended (along the field line) Floquet-type modes is observed [8,11]. The spectrum of electrostatic fluctuations shows a sub-ρ_i inertial range (where ρ_i is the ion Larmor radius) reminiscent of the $\rho_i k_y^{-10/3}$ [20] previously conjectured for tokamaks [18]. The regime is accessible through a variation of the ion temperature gradient only. Close to marginality, the saturation process features the coexistence of the primary Floquet-type source of turbulence, and extended radial structures that characterize the far-from-marginal (fluidlike) turbulence. As temperature gradients approach marginal values, a nearly total suppression of turbulence (cause of the Dimits shift [15]) is not observed. Its absence is attributed to the peculiar structure of marginal turbulence, which is less extended radially and therefore less prone to shearing by the zonal-flow-generated $\mathbf{E} \times \mathbf{B}$ flows. The practical consequences of this result are quite important since this implies that W7-X might feature a rather low nonlinear critical gradient (if one at all), which can limit performance. The observation of a strong dependence on the electron to ion temperature ratio in the turbulence levels of W7-X [9] seems to indicate that indeed the device operates close to marginality. The access to higher performance will necessarily rely on a deeper study of the type of turbulence reported here. A first step in that direction would be taken by simulating the whole plasma surface.

[1] A. Dinklage, C. Beidler, and the Wendelstein 7-X team, Nat. Phys. **14**, 855 (2018).

[2] S. A. Bozhenkov, Y. Kazakov, O. P. Ford, M. N. A. Beurskens, J. Alcusón, J. A. Alonso, J. Baldzuhn, C. Brandt, K. J. Brunner, H. Damm, Nucl. Fusion **60**, 066011 (2020).

[3] C. D. Beidler, Smith, A. H. M. Alonso, T. Andreeva, J. Baldzuhn, M. N. A. Beurskens, M. Borchardt, S. A. Bozhenkov, K. J. Brunner, H. Damm *et al.*, Nature (London) **596**, 221 (2021).

[4] J. M. Canik, D. T. Anderson, F. S. B. Anderson, K. M. Likin, J. N. Talmadge, and K. Zhai, Phys. Rev. Lett. **98**, 085002 (2007).

[5] B. Geiger, T. Wegner, C. Beidler, R. Burhenn, B. Buttenschön, R. Dux, A. Langenberg, N. Pablant, T. Pütterich, Y. Turkin *et al.*, Nucl. Fusion **59**, 046009 (2019).

[6] Th. Wegner, J. A. Alcusón, B. Geiger, A. von Stechow, P. Xanthopoulos, C. Angioni, M. N. A. Beurskens, L.-G. Böttger, S. A. Bozhenkov, K. J. Brunner *et al.*, Nucl. Fusion **60**, 124004 (2020).

[7] M. Beurskens, S. Bozhenkov, O. Ford, P. Xanthopoulos, A. Zocco, Y. Turkin, A. Alonso, C. Beidler, I. Calvo, D. Carralero *et al.*, Nucl. Fusion **61**, 116072 (2021).

[8] A. Zocco, P. Xanthopoulos, H. Doerk, J. W. Connor, and P. Helander, J. Plasma Phys. **84**, 715840101 (2018).

[9] D. Carralero, T. Estrada, E. Maragkoudakis, T. Windisch, J. A. Alonso, M. N. A. Beurskens, S. A. Bozhenkov, I. Calvo, H. Damm, O. P. Ford *et al.*, Nucl. Fusion **61**, 096015 (2021).

[10] M. Barnes, F. Parra, and M. Landreman, J. Comput. Phys. **391**, 365 (2019).

[11] B. J. Faber, M. J. Pueschel, J. H. E. Proll, P. Xanthopoulos, P. W. Terry, C. C. Hegna, G. M. Weir, K. M. Likin, and J. N. Talmadge, Phys. Plasmas **22**, 072305 (2015).

[12] L. I. Rudakov and R. Z. Sagdeev, Dokl. Akad. Nauk CCCP **138**, 581 (1961).

[13] B. Coppi, M. N. Rosenbluth, and R. Z. Sagdeev, Phys. Fluids **10**, 582 (1967).

[14] B. N. Rogers, W. Dorland, and M. Kotschenreuther, Phys. Rev. Lett. **85**, 5336 (2000).

[15] A. M. Dimits, G. Bateman, M. A. Beer, B. I. Cohen, W. Dorland, G. W. Hammett, C. Kim, J. E. Kinsey, M. Kotschenreuther, A. H. Kritz *et al.*, Phys. Plasmas **7**, 969 (2000).

[16] E. A. Frieman and L. Chen, Phys. Fluids **25**, 502 (1982).

[17] G. Roberg-Clark, G. Plunk, and P. Xanthopoulos, J. Plasma Phys. **87**, 905870306 (2021).

[18] M. Barnes, F. I. Parra, and A. A. Schekochihin, Phys. Rev. Lett. **107**, 115003 (2011).

[19] G. G. Plunk, P. Xanthopoulos, and P. Helander, Phys. Rev. Lett. **118**, 105002 (2017).

[20] A. A. Schekochihin, S. C. Cowley, W. Dorland, G. W. Hammett, G. G. Howes, G. G. Plunk, E. Quataert, and T. Tatsuno, Plasma Phys. Control. Fusion **50**, 124024 (2008).

[21] D. A. St-Onge, J. Plasma Phys. **83**, 905830504 (2017).

[22] D. R. Mikkelsen and W. Dorland, Phys. Rev. Lett. **101**, 135003 (2008).

[23] Z. Lin, T. S. Hahm, W. W. Lee, W. M. Tang, and R. B. White, Science **281**, 1835 (1998).

[24] P. Xanthopoulos, H. E. Mynick, P. Helander, Y. Turkin, G. G. Plunk, F. Jenko, T. Görler, D. Told, T. Bird, and J. H. E. Proll, Phys. Rev. Lett. **113**, 155001 (2014).

[25] A. Bader, B. J. Faber, J. C. Schmitt, D. T. Anderson, M. Drevlak, J. M. Duff, H. Frerichs, C. C. Hegna, T. G. Kruger, M. Landreman *et al.*, J. Plasma Phys. **86**, 905860506 (2020).

[26] P. W. Terry, P.-Y. Li, M. J. Pueschel, and G. G. Whelan, Phys. Rev. Lett. **126**, 025004 (2021).